Influence of Ortho-H 2 Clusters on the Mechanical Properties of Solid Para-H 2

ARTICLE *in* JOURNAL OF LOW TEMPERATURE PHYSICS · MARCH 2010

Impact Factor: 1.02 · DOI: 10.1007/s10909-009-0055-0 · Source: arXiv

5 AUTHORS, INCLUDING:

Anthony C Clark
Stanford University
13 PUBLICATIONS **363** CITATIONS
SEE PROFILE

Zhigang Cheng
University of Alberta
11 PUBLICATIONS **106** CITATIONS
SEE PROFILE

Noname manuscript No.
(will be inserted by the editor)

A. C. Clark · Z. G. Cheng · M. Bowne · X. Lin · M. H. W. Chan

Influence of Ortho-H_2 Clusters on the Mechanical Properties of Solid Para-H_2

Received: date / Accepted: date

Abstract The quantum diffusion of ortho-H_2 impurities in solid para-H_2 has been investigated with a torsional oscillator technique. The unclustering dynamics of agglomerated impurities with increasing temperature are found to greatly affect the resonant period of oscillation. Based on the observed trends in both experimental data and complementary finite element calculations, we find that the oscillation period predominantly reflects changes in the solid's elastic response to the minute inertial stresses imposed on it. It is likely that the small but abrupt increase in the resonant period observed above 100 mK in high purity H_2 samples is due to the interplay between remnant ortho-H_2 impurities and dislocations, and not a signature of a supersolid to normal solid transition.

Keywords solid hydrogen · impurities · diffusion · supersolid

PACS 61.72.-y · 61.72.Hh · 61.72.J- · 61.72.Yx · 62.20.de · 67.80.ff · 67.80.K-

Support provided by NSF Grants DMR 0207071 and 0706339.

A. C. Clark · Z. G. Cheng · M. Bowne · X. Lin · M. H. W. Chan
Department of Physics, The Pennsylvania State University, University Park, Pennsylvania 16802, USA

A. C. Clark
E-mail: cctony1@gmail.com
Present address: Department of Physics, University of Basel, CH-4056 Basel, Switzerland

M. Bowne
Present address: FRABA Inc., Hamilton, New Jersey 08609, USA

X. Lin
Present address: Department of Physics, Massachusetts Institute of Technology, Cambridge, Massachusetts 02139, USA

1 Introduction

The condensed hydrogen isotopes belong to a unique class of solids, quantum crystals, having constituent particles that exhibit extremely large zero point fluctuations about their equilibrium lattice sites. For the lightest isotope, H_2, this motion can be as large as 18% the nearest neighbor distance [1], well above the value considered as a melting criterion for most materials. Consequently, even at zero temperature there is a finite overlap of particle wavefunctions between lattice sites. The concept that zero point motion allows crystalline defects to become delocalized at low temperature, and the conjecture that this could result in the coexistence of elasticity and superfluidity [2], launched a series of experiments on both the solid hydrogens and (the even more quantum mechanical) helium [3].

At present there is still no indication of such a "supersolid" phase existing in H_2, and only recently has there been any evidence for such a phase in ^{4}He [4]. The majority of experimental results on ^{4}He suggesting the existence of supersolidity have been carried out using a torsional oscillator (TO) technique [5]. The underlying idea is that of an Andronikashvili experiment, i.e., the response of fluid to an oscillatory driving force when it is confined to dimensions much less than the viscous penetration depth. Information about the superfluid fraction of the liquid can be readily acquired from the resonant period τ of the TO based on a simple two fluid model. The normal fluid is viscously clamped to the cell, while the inherent zero viscosity of the superfluid component allows it to decouple from the system, thereby decreasing τ by an amount proportional to the superfluid mass. The story is more complicated for solids since the measured response also depends on the mechanical properties of the sample [6]. The most severe implication in regard to ^{4}He experiments is the possible lack of supersolidity altogether. However, a number of experiments and analysis tend to suggest otherwise [7,8,9,10,11,12, 13,14]. In one of our own works [11], we used a finite element method (FEM) to calculate the effect that changes in the solid ^{4}He elastic moduli would have on the TO resonant period. Combining these calculations with experiment we could extract the increase in the shear modulus G necessary to explain the phenomenon. In almost all cases the enhancements were completely nonphysical, and always found to be greater than that which has been measured [14,15]. Analogously, it was found that viscoelastic [10] and/or glassy [13] behavior can most probably only account for a small fraction of the period shifts observed.

In this paper we carry out a similar FEM analysis of data from earlier TO measurements on solid H_2, some of the latter of which was presented in [16]. Our previous study was part of a search for supersolidity in H_2. Interestingly, we observed an anomalous resonant period shift below $\sim$100 mK that depended on the concentration x of remnant ortho-H_2 (o-H_2) impurities. However, this apparent mass flow was found to be inconsistent with the notion of supersolidity during a blocked annulus the control experiment (see Sects. 3 and 4) [7,8].

A plethora of studies exist on defect (impurity) diffusion in hydrogen crystals in the temperature range 25 mK $< T <$ 4 K [17,18,19]. The variety

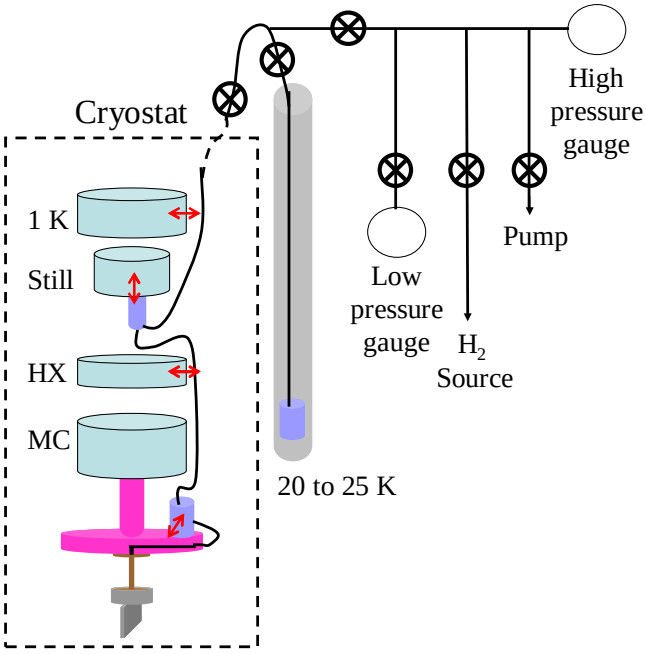

Fig. 1 Gas handling system that enabled the growth of H_2 with $x < 0.005$. The first stage of OP conversion is carried out at 20 K in a column separate from the dilution refrigerator. H_2 is condensed into the cell from the column. The lower conversion chambers in the capillary system are typically held around 15 K during sample growth. A final conversion "filter" just at the entrance to the torsion rod was made by filling the capillary within the bottom stage with FeO(OH).

of experimental techniques vary from "direct" detection methods such as nuclear magnetic resonance (NMR) of the different molecular, atomic and ionic spins in samples, to "global" detection of thermodynamic properties that are not only affected by diffusion itself but also by the final clustered state of o-H_2 that is favorable below 1 K. These latter studies typically involved monitoring the evolution of pressure, specific heat, thermal conductivity, etc. following abrupt temperature changes. Other experiments have concentrated on the mechanical properties of hydrogen crystals. Anomalous plasticity and creep of solid hydrogen samples have been observed below ∼5 K, and found to be quite sensitive to crystal quality and purity [20,21,22,23]. However, these very interesting investigations have been limited to stresses amplitudes ($\sigma > 500$ Pa) much higher than in TO measurements (between 20 and 400 mPa in this work) and $T > 1$ K, where quantum diffusion of o-H_2 impurities does not lead to clustering. Here we explore effects of impurities on the oscillatory response of solid H_2 under very low stress and in the temperature regime where impurity clustering enabled by quantum diffusion of spins is significant.

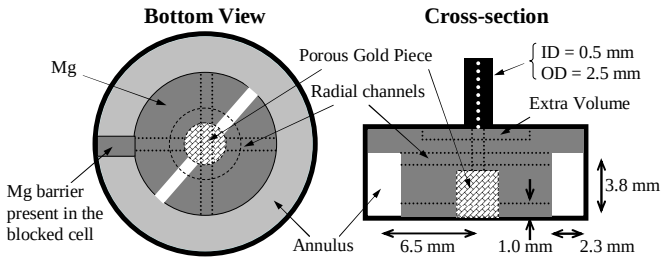

Fig. 2 Internal geometry of the open and blocked annulus TOs. The porous gold layer constitutes 2% of the total cell volume, and negligible rotational inertia. It was made by leaching Ag out from a machined AgAu cylinder, which is 2.5 mm in diameter and 3.3 mm tall. The resonant periods of the open and blocked cell TOs are 709,693 ns and 703,943 ns, respectively.

2 Samples

Three different varieties of hydrogen were used in these experiments: HD-depleted H_2 gas, ultra high purity (UHP) H_2 gas, and UHP HD gas. The isotopic compositions were $n < 10$ppm HD and/or D_2, 205±5 ppm HD [24] and $< 2\%$ H_2 and/or D_2, respectively. The bulk of the measurements were carried out on HD-depleted samples. A schematic of the capillary system used to grow samples is given in Fig. 1. Drawings depicting the inner cell of the TOs used in these experiments are shown in Fig. 2.

Apart from isotopic impurities, one can also speak of spin impurities. The two lowest rotational energy levels of the H_2 molecule are the para- and ortho- states, having $J = 0$ and 1, respectively. The asymmetry of the spin wave function for $J = 1$ requires that the spatial wave function also be asymmetric. Thus, o-H_2 impurities distort the surrounding lattice, which is made up of spherically symmetric p-H_2 molecules. Below 4 K the equilibrium concentration x_{eq} of o-H_2 is essentially zero. However, since the ortho-to-para (OP) conversion rate in the solid is very slow the most efficient way to produce samples with a small x is by exposing the liquid to a high surface area, magnetic material prior to crystallization. Thus, H_2 was first condensed into a column that housed a 40 cm^3 chamber partially filled with FeO(OH). The entire column was immersed in a storage dewar of liquid ^{4}He. The temperature of the inner chamber was stable at any fixed height above the surface of liquid ^{4}He. Prior to making solid samples the H_2 liquid was kept at 15 K for several hours or even overnight, at which temperature $x_{eq} \sim 10^{-4}$. To condense H_2 into the cell the temperature of the column was raised to between 20 and 25 K, where the vapor pressure is > 1 bar and $10^{-4} < x_{eq} < 10^{-2}$. For HD samples the gas was directly condensed into the cell.

Since OP conversion is an exothermic process, the average x for each sample in the torsion bob was determined by keeping the mixing chamber at 20 mK and measuring the temperature difference across the torsion rod. Based on this measurement and the thermal conductance of the Be-Cu torsion rod, we could infer the power being emitted during OP conversion, and hence the

initial concentration x_0 (and all subsequent x). Simply, we used the relation

$$\frac{\kappa_{BeCu} A \Delta T}{l} = \frac{U k x_0^2}{(1 + k x_0 t)^2} \tag{1}$$

where the heat of conversion $U = 1.06$ kJ mol^{-1}, the reaction rate k = 1.9% h^{-1}, and the thermal conductivity of BeCu K_{BeCu} was measured in the empty cell and found to agree extremely well with literature [25]. The smallest measurable temperature gradient of $\sim$0.1 mK corresponds to $x = 0.005$.

3 Experimental Results

Upon cooling H_2 samples to 20 mK, one to two weeks were allowed for equilibration, during which time τ dropped smoothly until finally stabilizing to within a drift of < 0.05 ns per day. The drift was completely halted by raising the temperature to 40 mK. After what was considered complete "equilibration" at 40 mK, T was raised in successive steps, for each of which τ was measured as a function of time. When the temperature sweep was complete the system was returned to 20 mK and allowed to re-equilibrate prior to a new scan. Since no long relaxation times were observed for HD samples, the rate of data acquisition was only limited by thermalization.

Several datasets corresponding to different hydrogen samples of annular geometry are shown in Fig. 3a. All samples were grown and measured in the TO from [16]. Since we are interested in changes to τ following an increase in temperature, constant offsets have been subtracted from each trace such that they all coincide at 0 K. The temperature dependence of the relative period shift $\Delta\tau$ between 150 mK and 1 K is approximately linear for the empty cell, HD sample, and $x = 0.15$ H_2 sample. A small deviation from linearity at the lowest temperatures is typical of BeCu TOs, as is the enhanced T-dependence (steeper slope) for TOs containing some amount of condensed gas. The second effect is not entirely understood, but has been observed in both solid ^{4}He experiments and studies of thin absorbed ^{4}He films [26]. The lowest temperature of 150 mK reached for the $x = 0.15$ sample is due to the large OP heat of conversion continually generated.

There are qualitatively different features found in data from H_2 samples with lower ortho-concentration. First, there is a period shift centered around 100 mK in each sample, which increases in size with decreasing x. Second, there is an additional deviation above 500 mK from the expected linear temperature dependence of $\Delta\tau$. The third and most striking difference, which cannot be extracted from Fig. 3, is the existence of long equilibration times at certain temperatures.

We investigated the temperature dependence of these relaxation times t_O, which are displayed for a number of samples in Fig. 4. The time dependence of the period was not exponential in many instances (e.g., see the "82 mK" trace in Fig. 3 inset of [16]). Since complete equilibration was obtained for $T > 60$ mK we could manually extract the time necessary to reach the e^{-1} value of each individual period shift following every temperature step. The

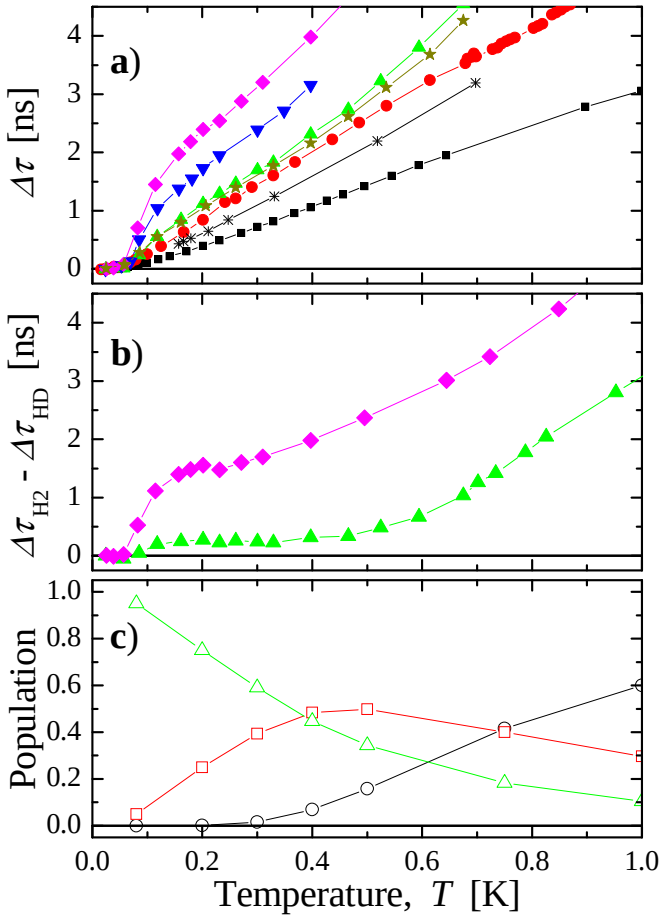

Fig. 3 a) T-dependence of $\Delta\tau$ for (black squares) the empty TO and the cell with (red circles) 91% filling of HD, (black asterisks) 88% filling of H_2 with $x = 0.15$, (brown stars) 83% filling of H_2 with $x = 0.025$, (green triangles) 83% filling of H_2 with $x = 0.02$, (blue inverted triangles) 68% filling of H_2 with $x < 0.005$, and (magenta diamonds) 88% filling of H_2 with $x < 0.005$. All datasets have been shifted vertically to match at $T = 0$ K for easy comparison. b) $\Delta\tau$ for (green triangles) 83% filling of H_2 with $x = 0.02$ and (magenta diamonds) 88% filling of H_2 with $x < 0.005$, after subtracting the T-dependence of $\Delta\tau$ for the HD sample. Although the low temperature feature appears to be of similar nature to that in solid ^{4}He experiments [7], it is not due to the onset of superfluidity [16]. c) Relative population of (black open circles) singles, (red open squares) pairs and (green open triangles) triangles is shown for $x = 0.01$. The curves are taken from [31] and are based on a simple statistical model.

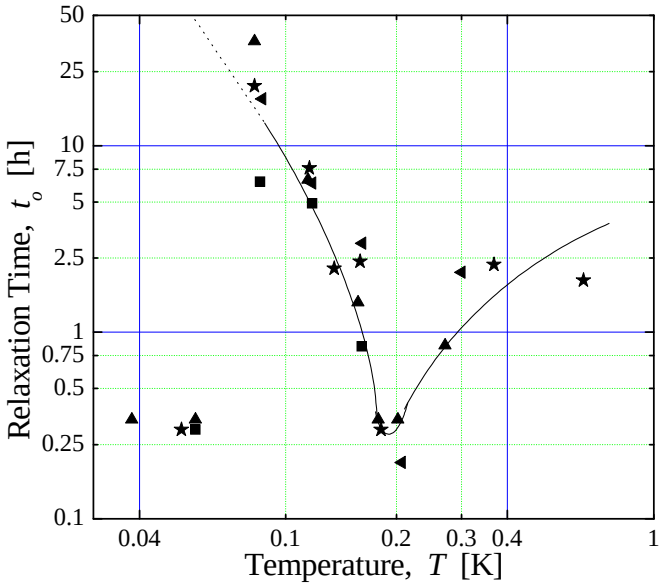

Fig. 4 T-dependence of t_O extracted from the time evolution of $\Delta\tau$. Data are taken from a number of different samples ($x < 0.025$) and stress amplitudes ($10 < \sigma < 400$ mPa). Below 60 mK the short t_O values measured may reflect the thermal equilibration time, whereas the true configurational relaxation times of o-H_2 are too long to be measured. As T increases from 80 and 180 mK the breakup of large o-H_2 clusters into pairs will occur at faster rates, shortening the time necessary for equilibration. For $T > 200$ mK the picture is further complicated as pairs begin to dissociate. At high enough temperature t_O will only depend on the motion of single o-H_2 molecules.

overall behavior was the same for all samples in three different TOs and for all concentrations in the range studied, $\sim 5\times10^{-3} < x < 0.025$. There was also no definitive dependence found on oscillation amplitude (i.e., rim velocity or inertial stress [11]), which was varied by a factor of ten. For all samples τ appeared to equilibrate quickly for 40 mK $\leq T \leq$ 60 mK. A more likely, alternative interpretation is that t_O was so long that the drift in the period measurement was hidden in the noise, and that true thermodynamic equilibrium was not achieved for $T < 60$ mK. Increasing the temperature further (above 60 mK) revealed extremely slow relaxation of τ. Near and above 180 mK it was found that the t_O shortened to less than the thermal equilibration time. Slow relaxation resumed at $T > 500$ mK, but data was not obtained close enough to equilibrium to determine t_O. An approximate lower limit is $\sim$5 h.

The internal dissipation Q^{-1} of the TO was also monitored, simultaneously with the period. Several traces are shown in the Fig. 5. The empty cell background is roughly linear over the entire temperature range, but exhibits a kink in the slope near 75 mK, above which the dependence is weaker. The presence of a H_2 sample increases the dissipation in the system. This excess dissipation ΔQ^{-1} is displayed in the bottom panel of the figure. The devia-

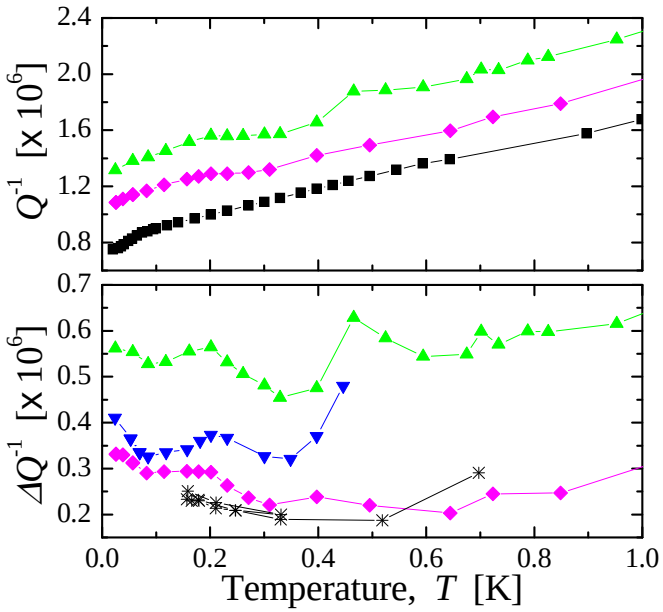

Fig. 5 Dissipation during oscillation. The legend is identical to that in Fig. 3. In the bottom panel the empty cell background has been subtracted. The excess dissipation due to H_2 depends on T, increasing over temperature intervals during which a large degree of cluster dissociation is believed to occur.

tions from the empty cell background, which are more pronounced in samples with $x < 0.15$, will be discussed in Sect. 5.

Finally, in our earlier work [16] a blocked annulus control experiment was carried out [7,8] in order to ascertain whether the observed effect in solid H_2 is a signature of supersolidity. The purpose of the barrier in the annulus is to make the path of irrotational superflow much more tortuous, thus leading to a predictable decrement in the measurable supersolid fraction [27]. We observed very similar $\Delta\tau$ and t_O in the blocked annulus, clearly indicated that the period shift in H_2 is not related to supersolidity.

4 FEM Calculations

Since the internal geometries of the two TOs (see Fig. 2) from [16] are more complicated than in ^{4}He experiments [11], using precise cell dimensions resulted in very large numbers of elements and made simulation times unfeasible. Due to simplifications that had to be made, most of the analysis should be considered qualitative.

In Fig. 6a we highlight the three key components of the open annulus TO for the most geometrically accurate FEM model. It was necessary to neglect the filling channels and porous gold core (the latter of which was included in order to lower the hydrogen-metal thermal boundary resistance). Since

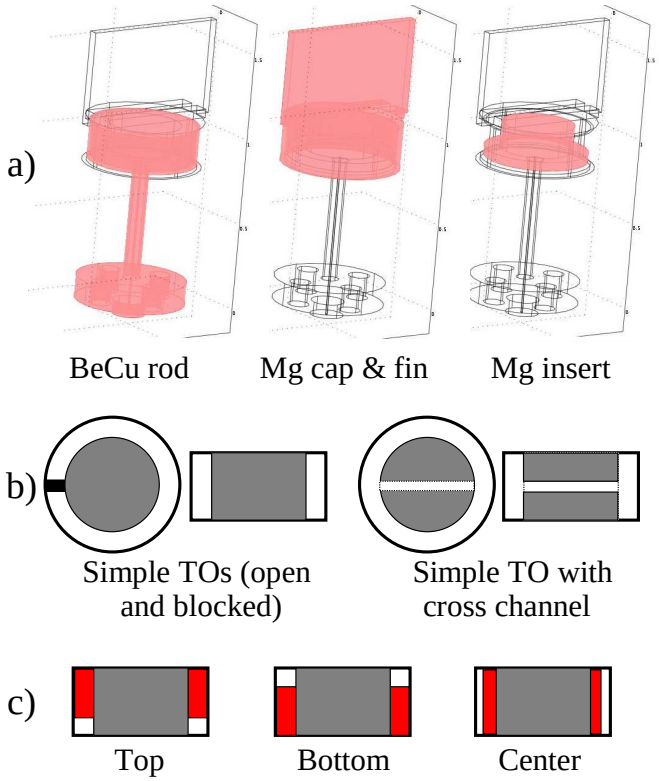

Fig. 6 a) The three main components making up the open annulus cell used in the first set of FEM calculations. Several of the internal features, such as the cross channels and porous gold piece (see Fig. 1), had to be removed. b) Top and side views of the hydrogen space within the abridged TOs used for most calculations. The open and blocked annulus TOs were simplified even further by replacing the Mg insert from (a) with a Mg cylinder. The simplified open annulus was made slightly more complex in one series of calculations by adding a cross channel. To keep τ fixed around 700,000 ns for all TOs (and matched to that in (a)) the outer Mg cap and fin were adjusted in size. c) Schematic of the three different distributions of H_2 within the cell that were modeled. This effect was investigated using the annulus cell from (a).

the insertion of a block in the annulus also increased the element number above our simulation ability, FEM calculations using even simpler internal geometries were necessary (see Fig. 6b). The geometry of the TOs used in these calculations were designed to have the same annular dimensions and similar resonant periods to the experimental values. One cross channel (see Fig. 6b) was also included in some calculations. In addition to altering the dimensions for the metal components of the TOs, we also investigated the effects from three different H_2 filling geometries: top, bottom and center (see Fig. 6c). These configurations were used for three different filling factors (i.e., period shifts due to different samples normalized by the maximum possible H_2 mass loading): 50%, 80% and 90%.

The FEM results are listed in Tables 1 and 2. The primary observations are the following: 1) calculated period shifts $\Delta\tau_{FEM}$ caused by decreases in the shear modulus of H_2 do not depend strongly on the distribution of H_2 within the cell, but rather on the sample filling factor (this has also been observed experimentally); 2) these same shifts are almost completely unaffected by the presence of a cross channel; 3) the shift is essentially the same for open and blocked annulus geometries; 4) changes to the bulk modulus K have little or no effect on both the open and blocked annulus TOs.

5 Discussion

The long relaxation times displayed in Fig. 4 exist at similar temperatures and are of similar magnitude to those from NMR studies of dilute ortho-para mixtures, which have been identified with the clustering of o-H_2 molecules (mostly into pairs) following a sharp drop in T [18,19]. The impurities effectively travel throughout the lattice via the transfer of $\hat{\mathrm{J}}$ from molecule to molecule rather than by particle exchange, thus it is spin (rather than mass) diffusion. This process is called resonant OP conversion [28]. Similar timescales are also observed for the restoration of isolated singles when pairs breakup during subsequent warming of the sample. On the contrary, Schweizer *et al.* found growth and decay times of o-H_2 pairs to exhibit considerable hysteresis when crystals were held below ∼50 mK for 10 h or more [29]. Since diffusion rates for both singles and pairs are enhanced below 100 mK formation of larger clusters will occur. These triangles, etc. are essentially immobile since they cannot propagate by the same resonant OP mechanism responsible for single and pair diffusion [30]. Once such a configuration has formed it appears, based on the lack of any observable pairs or singles, to remain frozen in for days even upon warming to 300 mK [29]. The rate of pair formation increases at higher T. For example, the presence of pairs was detected by Schweizer *et al.* following a 40 h "anneal" at 600 mK.

It is therefore important to point out the difference of the present investigation from the majority of earlier works. In previous studies the initial state was prepared at high temperature where the number of singles dominates over pairs and larger clusters [31,32]. Here, clustering is allowed to ensue for up to two weeks at 20 mK so that, according to decay times in the literature, no isolated o-H_2 singles [33] or pairs [34] remain in our samples at the beginning of each T sweep. After some weeks the overall configuration of o-H_2 will not change significantly since triangles and larger clusters cannot propagate. As the temperature of the TO is increased it is then possible to monitor the unclustering of these large agglomerations.

Before proceeding, it should be stressed that the short equilibration times in HD samples and the $x = 0.15$ H_2 sample [35], as well as the lack of dependence of t_O on x, are all consistent with our expectations if the phenomenon observed in dilute ortho-para mixtures is related to the unclustering and diffusion of spin impurities. Since these processes clearly affect the resonant period of the TO, an obvious question must be addressed: what physical property of hydrogen does the TO measure? In [16] we briefly discussed a

Table 1 FEM results for different TOs. To investigate the possible correlation between o-H_2 dynamics and the mechanical properties of the solid, τ was calculated for different values of the shear and bulk moduli. The period shifts, listed below (in nanoseconds) for different TOs, correspond to decreases in G or K by 10%.

Modulus	Annulus	Simple Annulus	Simple Block	Simple Channel
G	0.164	0.716	0.697	0.733
K	–	0.028	0.028	–

Table 2 The effect of hydrogen distribution within the cell. $\Delta\tau_{FEM}$ were calculated for different sample filling factors and configurations (see Fig. 6c). The period shifts, in nanoseconds, correspond to a 10% decrease in G.

Filling Factor	Top	Bottom	Center	$\Delta\tau_{FEM}$[Bottom]/$\Delta\tau_{FEM}$[Full]
50%	0.072	0.086	0.069	52.4%
80%	0.129	0.128	0.109	78.0%
90%	–	0.133	–	81.1%

few possibilities. For example, the wetting properties of H_2 [36] could be influenced by the local OP composition. It is difficult to predict what consequences this would have on the resonant period measurement. However, in the case of slippage occuring between the sample and cell walls one would expect corresponding period shifts to increase dramatically with oscillation amplitude and eventually become entirely irreproducible upon cycling, contrary to our observations.

We also pointed out that the moment of inertia is sensitive to the radial density profile of a H_2 sample, and thus rearrangement of impurities within the cell could reduce or enhance the resonant period. Since the density of o-H_2 is only 1.7% higher than that of p-H_2 [17], ortho-concentrations less than a few percent cannot influence the moment of inertia of H_2 (by clustering at small or large radii within the cell) by more than a few parts in 10^4 (and thus the period by a few parts in 10^9). Although this is similar to the observed $\Delta\tau$ it is an extreme case that is clearly nonphysical in view of tunneling probabilities of triangles and larger clusters [30].

Since most of the samples did not entirely fill the cell, one can also consider the thermal contraction of H_2. The molar volume change from the freezing point T_m down to zero temperature, 1.1% [37], can decrease the outer radius of a confined ring of H_2 by no more than ∼0.37%, and thus the moment of inertia by ∼2% for the given cell dimensions. This percentage of the mass loading sets an upper limit of ∼60 ns. For all hydrogen samples τ did drop by several tens of nanoseconds between the freezing point and low T. However, contraction should only affect the resonant period between $0.5\,T_m$ and T_m, whereas we observed large changes even when cooling below 4 K.

Physical quantities that also change significantly below the freezing point are the bulk and shear moduli, increasing by at least 10% or 20% [37,38, 39]. Although the majority of stiffening is expected to occur just below T_m, the pinning of dislocation motion (e.g., in solid ^{4}He [40,41]) can affect the finite frequency, mechanical response of crystals [11,14,42]. For solid ^{4}He the

primary pinning mechanism is the binding energy (between 300 mK and 1 K) between dislocations and ^{3}He impurities. In the zero temperature limit all available binding sites around the dislocation network are occupied by ^{3}He. The density of isotopic impurities in the vicinity of dislocations decreases at finite T due to the thermally activated evaporation of ^{3}He. Once freed of ^{3}He, the dislocation lines suffer from very few scattering processes and can therefore vibrate freely and very effectively soften the crystal [14,15]. Such a phenomenon in H_2 crystals, which have the same hexagonal-close-packed (hcp) structure and similar dislocation densities ($\sim 10^8$ cm^{-2} [43]) as ^{4}He, could result in a temperature dependent resonant period well below T_m. The interaction strength between dislocations and HD impurities is $\sim$5 K and is much larger than for ^{3}He in solid ^{4}He. However, for both singles and pairs of o-H_2 molecules the calculated binding energy is between 400 mK and 1 K for different types of dislocations. One must therefore recognize the potential importance of the concentration and mobility of o-H_2 on τ even at milliKelvin temperatures.

Clearly, both singles and pairs can escape from potential wells around dislocation lines within the sample if T is sufficiently high (tens to hundreds of milliKelvin). However, two other very important prerequisites are that these types of impurities are actually present in the sample and that they are mobile. For instance, in thermodynamic equilibrium the relative population of singles is negligible below $\sim$300 mK [31,32]. At higher temperature their number increases, as does their mobility. On the contrary, the population of pairs increases only up to $T \sim 500$ mK. Moreover, they are only highly mobile below $\sim$100 mK. With this information in mind the interpretation of the data in Fig. 3 is as follows. Below 60 mK the o-H_2 configuration is quasi-static. Any small drifts in τ are likely accounted for by the continual OP conversion process. That is, the flipping of one spin can cause a triangle to become a pair, which can diffuse. The o-H_2 impurities are otherwise immobile. Each of the triangles and larger clusters serve as pinning sites for dislocations. However, above 60 mK a finite number of pairs is thermodynamically favorable (see Fig. 3c), and thus the gradual breakup of clusters will ensue. Since all of these pairs (both in-plane and out-of-plane [34]) are mobile for $T > 60$ mK [30], they need not be bound to the dislocation network. This can lower the effective elastic moduli. The sharp increase in $\Delta\tau$ at 60 mK is consistent with a growing number of propagating pairs. This begins to level off above 100 mK as pair mobility drops, limiting their escape rate from various binding sites. The $\Delta\tau$ observed in this temperature range will be smaller in samples with higher ortho-concentrations since the crossover from network-pinning to impurity-pinning [40,41,42] occurs at higher T. Above 400 mK the slope of $\Delta\tau$ in Fig. 3 increases again and is most likely due to the enhanced population of isolated o-H_2 molecules in the sample. Since these singles become more mobile between 300 mK and > 1 K, they will continue to successfully evaporate from dislocation lines. Thus, the crystal should continue to soften with increasing T over this entire temperature interval, as is observed.

There are several remarks to make concerning the expected magnitude of $\Delta\tau$ stemming from changes to elastic moduli. First, one clear conclusion based on FEM calculations is that only changes in the shear (versus bulk)

modulus could be reflected in resonant period. This appears intuitive from the symmetry within the cell of the open annulus TO, but is not obvious for the blocked annulus cell. The nearly identical behavior expected from shear modulus changes for both the open and blocked annulus configurations (see Table 1) was already noted in [11] as strong evidence for a supersolid ^{4}He phase. In the present work the same test not only serves as very solid evidence *against* a supersolid H_2 phase, but demonstrates the qualitative agreement between experiments and FEM calculations.

Second, the influence of x might be expected to oppose that displayed in Fig. 3. That is, it is appropriate to ask whether or not greater amounts of impurities produce larger period shifts. In the simplest picture presented here $\Delta\tau$, mainly depends on the difference in G for the two cases of "all dislocations pinned" ($T = 0$ K) and "all dislocations freely vibrating" (limited only by intersecting dislocation lines). This quantity is independent of x, but depends on sample quality (dislocation density). We actually observe a larger effect at lower concentrations that, as mentioned above, probably reflects the lower impurity-pinning crossover temperature in samples with lower ortho-concentrations [42], but also will be influenced by the variations the dislocation network from sample to sample.

Third, although the model shown in Fig. 6a is the most similar in design to the experimental TOs, the absolute accuracy of $\Delta\tau_{FEM}$ values obtained from it is uncertain. For instance, the difference between using it and using the simpler versions in Figs. 6b and 6c is a factor of almost five in magnitude. This appears somewhat contrary to the fact that small changes to the internal geometry (tested with the simplified TOs) do not significantly alter $\Delta\tau_{FEM}$. Taking the most dramatic result from Table 1 ($\Delta\tau_{FEM} = 0.733$ ns per 10% decrease in G), we find that between 0 and 200 mK (1 K) the shear modulus must drop by 20% (68%) to explain the 1.5 ns (5 ns) difference between the H_2 and HD curves plotted in Fig. 3b. Some of the discrepancy between experiment and FEM analysis could be accounted for by viscoelasticity [10] and/or glassy behavior [6], which can be extracted from features in the dissipation. Further, it may be that the additional components (Mg, porous gold, etc.) within the cell are less coupled to the TO when H_2 softens. This glue-like effect could enhance $\Delta\tau$. We note that although we are unable to quantitatively simulate the effect, it would be straightforward to repeat the experiment with a very simple TO design.

The same physical picture can be applied to Fig. 4. Relaxation times are extremely long below 60 mK since there are very few mobile impurities. Above this temperature the slow dissociation of clusters and the diffusion of pairs into some quasi-equilibrium configuration will result in long relaxation times. The decrease in t_O as T increases toward 200 mK could reflect the increasing dissociation rate of clusters. As T is raised further the motion of pairs will slow down and the relaxation process will become dominated by the breakup into singles, their liberation from dislocations, and their faster diffusion above several hundred milliKelvin.

In TO experiments on ^{4}He the dissipation peak (unlike the period shift) can be entirely accounted for by glassy [6,13] or viscoelastic [10] effects. Such behavior is most likely linked to the influence of ^{3}He-dislocation interactions

[40,41,42] on the shear modulus [11,15]. In H_2 there are at least two processes that could cause dissipation for $T < 1$ K. First, there is the possible unbinding of o-H_2 molecules from dislocations, for which we expect ΔQ^{-1} to be centered around the associated $\Delta\tau$. Second, there is the dissociation of clusters, which should also affect the mechanical response of the solid. By comparing Fig. 3b with Fig. 5, we find that none of the "peaks" in dissipation are centered around large $\Delta\tau$. For example, the peak at 200 mK occurs between the period shifts at $\sim$80 and $>$ 300 mK. We speculate that the dissociation of o-H_2 clusters, marked by large relative populations of pairs and singles (see Fig. 3c), is primarily responsible for the regions of enhanced dissipation.

6 Conclusions

The mechanical response of solid hydrogen samples to extremely low stresses has been measured using a torsional oscillator. A careful analysis of the data, complemented by FEM calculations, confirm the conclusion of [16] that the change in the TO resonant period is not related to the onset of superfluidity in solid H_2. Rather, $\Delta\tau$ is found to reflect changes in the shear modulus of the sample. The most prominent shift occurs between 60 and 180 mK and most likely corresponds to the breakup of large o-H_2 clusters into triangles and pairs of molecules. Further softening of the solid occurs at higher temperature as clusters gradually separate into isolated molecules. The temperature intervals over which the unclustering takes place is complemented by enhanced internal dissipation.

Acknowledgements Thanks to P. J. Polissar and C. Turich for assistance with mass spectrometry. We are particularly grateful to H. Meyer for his advice, numerous communications on solid hydrogen and warm encouragements.

References

1. M. Nielsen, Phonons in solid hydrogen and deuterium studied by inelastic coherent neutron scattering, Phys. Rev. B **7**,1626-1635 (1973)
2. A. F. Andreev, I. M. Lifshitz, Quantum theory of defects in crystals, Sov. Phys. JETP **29**, 1107-1113 (1969)
3. M. W. Meisel, Supersolid ^{4}He: An overview of past searches and future possibilities, Physica B **178**, 121-128 (1992)
4. E. Kim, M. H. W. Chan, Probable observation of a supersolid helium phase, Nature **427**, 225-227 (2004)
5. J. E. Berthold, D. J. Bishop, J. D. Reppy, Superfluid transition of ^{4}He films adsorbed on porous vycor glass, Phys. Rev. Lett. **39**, 348-352 (1977)
6. Z. Nussinov, A. V. Balatsky, M. J. Graf, S. A. Trugman, Origin of the decrease in the torsional-oscillator period of solid ^{4}He, Phys. Rev. B **76**, 014530 (2007)
7. E. Kim, M. H. W. Chan, Observation of superflow in solid helium, Science **305**, 1941-1944 (2004)
8. A. S. C. Rittner, J. D. Reppy, Probing the upper limit of nonclassical rotational inertia in solid helium-4, Phys. Rev. Lett. **101**, 155301 (2008)
9. Y. Aoki, J. C. Graves, H. Kojima, Oscillation Frequency Dependence of nonclassical rotation inertia of solid ^{4}He, Phys. Rev. Lett. **99** 015301 (2007)

10. C.-D. Yoo, A. T. Dorsey, Theory of viscoelastic behavior of solid ^{4}He, Phys. Rev. B **79**, 100504(R) (2009)
11. A. C. Clark, J. D. Maynard, M. H. W. Chan, Thermal history of solid ^{4}He under oscillation, Phys. Rev. B **77**, 184513 (2008)
12. Y. Aoki, M. C. Keiderling, H. Kojima, New dissipation relaxation phenomenon in oscillating solid ^{4}He, Phys. Rev. Lett. **100**, 215303 (2008)
13. B. Hunt *et al.*, Evidence for a superglass state in solid ^{4}He, Science **324**, 632-636 (2009)
14. J. T. West, O. Syshchenko, J. R. Beamish, M. H. W. Chan, Role of shear modulus and statistics in the supersolidity of helium, Nature Physics advance online publication, 13 July 2009 (DOI 10.1038/nphys1337)
15. J. Day, J. R. Beamish, Low-temperature shear modulus changes in solid ^{4}He and connection to supersolidity, Nature **450**, 853-856 (2007)
16. A. C. Clark, X. Lin, M. H. W. Chan, Search for superfluidity in solid hydrogen, Phys. Rev. Lett **97**, 245301 (2006)
17. I. F. Silvera, The solid molecular hydrogens in the condensed phase: Fundamentals and static properties, Rev. Mod. Phys. **52**, 393-452 (1980)
18. H. Meyer, Quantum diffusion in solid H_2: A short review, Can. J. Phys. **65**, 1453-1462 (1987)
19. H. Meyer, Quantum diffusion and tunneling in the solid hydrogens (a short review), Low Temp. Phys. **24**, 381-392 (1998)
20. L. A. Alekseeva, I. N. Krupskii, Superplasticity of solid parahydrogen, Sov. J. Low Temp. Phys. **10**, 170-172 (1984)
21. A. N. Aleksandrovskii, E. A. Kir'yanova, V. G. Manzhelli, A. V. Soldatov, A. M. Tolkachev, Anomalies of the plastic deformation of solid parahydrogen, Sov. J. Low Temp. Phys. **13**, 623-624 (1987)
22. L. A. Alekseeva, A. V. Pustovalova, V. I. Khatuntsev, Yu. V. Butenko, Low-temperature unsteady creep of parahydrogen single crystals, Low Temp. Phys. **28**, 58-60 (2002)
23. L. A. Alekseeva, E. S. Syrkin, L. A. Vashchenko, Low-temperature plasticity and lattice dynamics of solid parahydrogen with an isotopic impurity, Phys. Solid State **45**, 1073-1078 (2003)
24. Mass spectrometry of UHP H_2 gas carried out at PSU consistently yielded HD impurity levels of 205 ± 5 ppm.
25. A. L. Woodcraft, Zirconium copper - a new material for use at low temperatures?, AIP Conference Proceedings **850**, 1691-1692, (2005)
26. G. Agnolet, D. F. McQueeney, J. D. Reppy, Kosterlitz-Thouless transition in helium films, Phys. Rev. B *39*, 8934-8958 (1989)
27. A. L. Fetter, Vortex nucleation in deformed rotating cylinders, J. Low Temp. Phys. **16**, 533-555 (1974)
28. R. Oyarzun and J. Van Kranendonk, Quantum diffusion in solid hydrogen and deuterium, Phys. Rev. Lett. **26**, 646-648 (1971)
29. R. Schweizer, S. Washburn, H. Meyer, A. B. Harris, NMR studies of single crystals of H_2: II. The spectrum of isolated ortho-H_2 pairs, J. Low Temp. Phys. 37, 309-341 (1979)
30. J. Van Kranendonk, Quantum diffusion of ortho-hydrogen pairs in solid parahydrogen, J. Low Temp. Phys. **39**, 689-699 (1980)
31. H. Meyer, Comments on two recent papers on solid H_2, Phys. Rev. **187**, 1173-1174 (1969)
32. I. Ya Minchina, M. I. Bagatskii, V. G. Manzhelli, A. I. Krivchikov, Quantum diffusion in hydgrogen, studied by calorimetric methods, Sov. J. Low Temp. Phys. **10**, 549-556 (1985)
33. X. Li, D. Clarkson, H. Meyer, Thermal conductivity and quantum diffusion in solid H_2, J. Low Temp. Phys. **78**, 335-349 (1990)
34. S. Washburn, R. Schweizer, H. Meyer, NMR Studies on single crystals of H_2: III. Dynamic effects, J. Low Temp. Phys. **40**, 187-205 (1980)
35. Mobility of o-H_2 is limited in less dilute mixtures. A crossover has been observed near $x = 0.07$. See J. F. Jarvis, H. Meyer, D. Ramm, Measurement of $(\partial P/\partial T)_V$ and related properties in solidified gases. II. Solid H_2, Phys. Rev. **178**, 1461-1471 (1969)

36. M. Sohaili, J. Klier, P. Leiderer, Triple-point wetting of molecular hydrogen isotopes, J. Phys. Condens. Matter **17**, S415-S428 (2005)
37. I. N. Krupskii, A. I. Prokhvatilov, G. N. Shcherbakov, Thermal expansion of solid parahydrogen, Sov. J. Low Temp. Phys. **9**, 42-45 (1983)
38. V. G. Manzhelii, B. G. Udovidchenko, V. B. Esel'son, Thermal expansion and isothermal compressibility of solid hydrogen in the premelting range under pressures up to 200 atm. A new phase transformation, Sov. J. Low Temp. Phys. **1**, 384-391 (1975)
39. J. K. Krause, C. A. Swenson, Direct measurements of the constant-volume heat capacity of solid parahydrogen from 22.79 to 16.19 cm^3/mole and the resulting equation of state, Phys. Rev. B **21**, 2533-2548 (1980)
40. I. Iwasa, H. Suzuki, Sound velocity and attenuation in hcp ^{4}He crystals containing ^{3}He impurities, J. Phys. Soc. Jpn. **49**, 1722-1730 (1980)
41. M. A. Paalanen, D. J. Bishop, H. W. Dail, Dislocation Motion in hcp ^{4}He, Phys. Rev. Lett. **46**, 664-667 (1981)
42. E. Kim *et al.*, Effect of ^{3}He impurities on the nonclassical response to oscillation of solid ^{4}He, Phys. Rev. Lett. **100**, 065301 (2008)
43. O. A. Korolyok, B. Ya. Gorodilov, A. I. Krivchikov, A. V. Raenko, A. Jezowski, Phonon scattering by structural defects in solid p-H_2 and in p-H_2-o-D_2 solutions, Low Temp. Phys. **27**, 504-508 (2001)